Drink. Water Eng. Sci. Discuss., 7, 27–57, 2014
www.drink-water-eng-sci-discuss.net/7/27/2014/
doi:10.5194/dwesd-7-27-2014

Open Access
Drinking Water
Engineering and Science
Discussions

A pipe network simulation model with dynamic transition between free surface and pressurized flow

J. Fernández-Pato and P. García-Navarro

LIFTEC (CSIC) – University of Zaragoza, C/María de Luna 5, 50018 Zaragoza, Spain

Received: 20 December 2013 – Accepted: 11 January 2014 – Published: 27 January 2014

Correspondence to: J. Fernández-Pato (jfpato@unizar.es)

Published by Copernicus Publications on behalf of the Delft University of Technology.

Abstract

Water flow numerical simulation in urban pipe systems is one of the topics that shows the need for surface flows and pressurized flows in steady and transient situations. The governing equations for both flow types are different and this must be taken into account in order to get a complete numerical model for solving transients. A numerical simulation model is developed in this work, capable of solving pipe networks mainly unpressurized, with isolated peaks of pressurization. For this purpose, a reformulation of the mathematical model through the Preissmann slot method is proposed. By means of this technique, a reasonable estimation of the water pressure is calculated in cases of pressurization. The numerical model is based on the first order Roe's scheme, in the frame of finite volume methods. It is adapted to abrupt transient situations, with subcritial and supercritical flows. The validation has been done by means of several cases with analytic solutions or empirical laboratory data. It has also been applied to some more complex and realistic cases, like junctions or pipe networks.

1 Introduction

Numerical simulation of pipe systems is characterized by the difficulty of setting a network to simulate both transitory and steady states. The water flow is mainly unpressurized, but the pipes have a limited storage capacity and could be drowned under exceptional conditions if the water level raises quickly. In these situations, the flux is pressurized and another mathematical model should be taken into account in order to solve the problem accurately.

A complete pipe system model should be able to solve steady and transient flows under pressurized and unpressurized situations and the transition between both flows (mixed flows). Most of the models developed primarly to study the propagation of hydraulic transients use schemes based on the Method of Characteristics (MOC) to solve both system of equations e.g., Gray (1954); Wiggert et al. (1977). This method trans-

DWESD

7, 27–57, 2014

form the continuity and momentum partial differential equations into a set of ordinary differential equations that are easier to solve. Although the MOC schemes can handle complex boundary conditions, interpolation is needed in some cases and they are not strictly conservatives. This result in diffusion of the wave fronts that makes waves arrive to the boundaries at a wrong time. Therefore, a new efficient numerical scheme is needed in order to solve accurately the wave front.

Mixed flow problems have been addressed in the last decades by several researchers under two main points of view. The first one consists of solving separately pressurized and shallow flows. Transitions between both flux types are treated as internal boundary conditions. This kind of models are more complex but capable to simulate sub-atmospheric pressures in the pipe. Other authors e.g., García-Navarro et al. (1993); León et al. (2009); Kerger et al. (2010) developed simulations applying the shallow water equations in a slim slot over the pipe (Preissmann slot method). The water level in the slot gives an estimation of the pressure of the pipe. The great advantage of this model is the use of one equation system for solving the complete problem. It has been widely used to simulate local transitions between pressurized/shallow flows but it is not so succesful for abrupt transitions e.g., Trajkovic et al. (1999) due to stability problems when the pipe width is replaced for the slot one. This fact results in a big difference between the wave speeds (from $\sim 10\,\mathrm{m\,s^{-1}}$ in shallow flow to $\sim 1000\,\mathrm{m\,s^{-1}}$ in pressurized flow). In order to solver this issue, the slot width could be increased, but it implies an accuracy loss in the results, due to the no-mass/momentum conservation.

This work is focused on the development of a simulation model capable to solve pipe system networks working mainly under shallow flow situations but exceptionally pressurized, so it is based on the second options previously mentioned. Hence, it is aimed to generalize the shallow water equations by means of the Preissmann slot method. The explicit first order Roe scheme has been used as numerical method for all the simulations.

DWESD
7, 27–57, 2014

J. Fernández-Pato and P. García-Navarro

The calculation times are not long so implicit methods or parallel computation have been dismissed. Fluxes and source terms have been treated by means of an upwind scheme García-Navarro et al. (2000).

2 Mathematical model

2.1 Shallow water equations

It is generally accepted that unsteady open channel water flows are governed by the 1-D shallow water or St. Venant equations. These equations represent mass and momentum conservation along the main direction of the flow and are a good description for most of the pipe-flow-kind problems. They can be written in a conservative form as follows:

$$\frac{\partial A}{\partial t} + \frac{\partial Q}{\partial x} = 0 \tag{1}$$

$$\frac{\partial Q}{\partial t} + \frac{\partial}{\partial x}\left(\frac{Q^2}{A} + gI_1\right) = gI_2 + gA(S_0 - S_f) \tag{2}$$

where A is the wetted cross section, Q is the discharge, g is the gravity acceleration, I_1 represents the hydrostatic pressure force term and I_2 accounts for the pressures forces due to channel/pipe width changes:

$$I_1 = \int_0^{h(x,t)} (h - \eta)\, b(x,\eta) \mathrm{d}\eta \tag{3}$$

$$I_2 = \int_0^{h(x,t)} (h - \eta) \frac{\partial b(x,\eta)}{\partial x} \mathrm{d}\eta \tag{4}$$

$$b = \frac{\partial A(x,\eta)}{\partial \eta} \tag{5}$$

The remaining terms, S_0 and S_f, represent the bed slope and the energy grade line (defined in terms of the Manning roughness coefficient), respectively:

$$S_0 = -\frac{\partial z}{\partial x}, \qquad S_f = \frac{Q|Q|n^2}{A^2 R^{4/3}} \tag{6}$$

where $R = A/P$, P being the wetted perimeter. The coordinate system used for the formulation is shown in Fig. 1. It is useful to rewrite the equation system in a vectorial form:

$$\frac{\partial \mathbf{U}}{\partial t} + \frac{\partial \mathbf{F}}{\partial x} = \mathbf{R} \tag{7}$$

where

$$\mathbf{U} = (A,Q)^T \tag{8}$$

$$\mathbf{F} = \left(Q, Q^2/A + gI_1\right)^T \tag{9}$$

$$\mathbf{R} = (0, gI_2 + gA(S_0 - S_f))^T \tag{10}$$

In those cases in which $\mathbf{F} = \mathbf{F}(\mathbf{U})$, when $I_2 = 0$, it is possible to rewrite the conservative system by means of the Jacobian matrix of the system:

$$\frac{\partial \mathbf{U}}{\partial t} + \mathbf{J}\frac{\partial \mathbf{U}}{\partial x} = \mathbf{R}, \qquad \mathbf{J} = \frac{\partial \mathbf{F}}{\partial \mathbf{U}} = \begin{pmatrix} 0 & 1 \\ c^2 - u^2 & 2u \end{pmatrix} \tag{11}$$

where c is the wave speed (analogous to the speed of sound in gases), defined as follows:

$$c = \sqrt{g\frac{\partial I_1}{\partial A}} \tag{12}$$

DWESD
7, 27–57, 2014

The system matrix can be made diagonal by means of its set of real eigenvalues and eigenvectors, which represent the speed of propagation of the information:

$$\lambda^{1,2} = u \pm c, \qquad \mathbf{e}^{1,2} = (1, u \pm c)^T \tag{13}$$

It is very common to characterize the flow type by means of the Froude number $Fr = u/c$ (analogous to the Mach number in gases). It allows the classification of the flux into three main regimes: subcritical $Fr < 1$, supercritical $Fr > 1$ and critical $Fr = 1$.

2.2 Water-hammer equations

The inmediate response to changes in pipe flow can be taken up by the elastic compressibility of both the fluid and the pipe walls. Unsteady flow in the pipe can be described by the cross-section integrated mass and momentum equations (Chaudhry et al., 1994):

$$\frac{\partial H}{\partial t} + v\frac{\partial H}{\partial x} + v\sin\theta + \frac{c_{\mathrm{WH}}^2}{g}\frac{\partial v}{\partial x} = 0 \tag{14}$$

$$\frac{\partial v}{\partial t} + v\frac{\partial v}{\partial x} + g\frac{\partial H}{\partial x} + \frac{4\tau_0}{\rho D} = 0 \tag{15}$$

in which $H(x,t)$ is the elevation of the hydraulic grade line, $v(x,t)$ is the local cross-section averaged flow velocity, D is the diameter, τ_0 is the boundary shear, typically estimated by means of a Manning or Darcy–Weissbach friction model. The magnitude c_{WH} represents the speed of an elastic wave in the pipe:

$$c_{\mathrm{WH}} = \sqrt{\frac{K/\rho}{1 + \frac{DK}{eE}}} \tag{16}$$

being e the pipe thickness and E, K the elastic modulus of the pipe material and fluid, respectively. By neglecting convective terms, it's possible to get a linear hyperbolic

DWESD
7, 27–57, 2014

J. Fernández-Pato and P. García-Navarro

equation system:

$$\frac{\partial H}{\partial t} + \frac{c_{\mathrm{WH}}^2}{g}\frac{\partial v}{\partial x} = 0 \tag{17}$$

$$\frac{\partial v}{\partial t} + g\frac{\partial H}{\partial x} + \frac{4\tau_0}{\rho D} = 0 \tag{18}$$

These equations conform a hyperbolic system, analogous to the shallow water equations, considering the pressure and the velocity as the conserved variables.

3 Preissmann slot model

The Preissmann slot approach assumes that the top of the pipe or closed channel is connected to a hypothetical narrow slot, open to the atmosphere, so the shallow water equations can be applied including this slot (see Fig. 2). The slot width is ideally chosen equaling the speed of gravity waves in the slot to the water hammer wavespeed, so the water level in the slot is equal to the pressure head level. This model is based on the previously remarked similarity between the wave equations which describe free surface/pressurized flows. The water hammer flow comes from the capacity of the pipe system to change the area and fluid density, so forcing the equivalence between both models requires that the slot stores as much fluid as the pipe would by means of a change in area and fluid density. The pressure term and the wavespeed for $A \leq bH$ are:

$$h = \frac{A}{b} \tag{19}$$

$$I_1 = \frac{A^2}{2b} \tag{20}$$

$$c = \sqrt{g\frac{\partial I_1}{\partial A}} = \sqrt{g\frac{A}{b}} \tag{21}$$

DWESD
7, 27–57, 2014

A pipe network simulation model

J. Fernández-Pato and P. García-Navarro

and for $A > bH$:

$$h = H + \frac{A - bH}{b_s} \tag{22}$$

$$I_1 = bH\left(\frac{A - bH}{b_s} + \frac{H}{2}\right) + \frac{(A - bH)^2}{2b_s} \tag{23}$$

$$c = \sqrt{g\frac{\partial I_1}{\partial A}} = \sqrt{g\frac{A}{b_s}} \tag{24}$$

The ideal choice for the slot width results in:

$$c_{\mathrm{WH}} = c \Rightarrow b_s = g\frac{A_{\mathrm{f}}}{c_{\mathrm{WH}}^2} \tag{25}$$

in which A_{f} is the full pipe cross-section.

4 Finite volume numerical model

4.1 Explicit first order Roe scheme

Roe scheme is based on a local linearization of the conserved variables and fluxes:

$$\delta\mathbf{F} = \tilde{\mathbf{J}}\delta\mathbf{U} \tag{26}$$

It is necessary to build an approximate Jacobian matrix $\tilde{\mathbf{J}}$ whose eigenvalues and eigenvectors satisfy:

$$\delta\mathbf{U}_{i+1/2} = \mathbf{U}_{i+1} - \mathbf{U}_i = \sum_{k=1}^{2}(\tilde{\alpha}_k\tilde{\mathbf{e}}_{\mathbf{k}})_{i+1/2} \tag{27}$$

$$\delta\mathbf{F}_{i+1/2} = \mathbf{F}_{i+1} - \mathbf{F}_i = \tilde{\mathbf{J}}_{\mathbf{i+1/2}}\delta\mathbf{U}_{i+1/2} = \sum_{k=1}^{2}(\tilde{\lambda}_k\tilde{\alpha}_k\tilde{\mathbf{e}}_{\mathbf{k}})_{i+1/2} \tag{28}$$

DWESD
7, 27–57, 2014

J. Fernández-Pato and P. García-Navarro

The $\tilde{\alpha}_k$ coefficients represent the variable variation coordinates in the Jacobian matrix basis. The eigenvalues and eigenvectors are expressed in terms of the average flux and wave speeds:

$$\tilde{\lambda}_k = (\tilde{u} \pm \tilde{c}), \qquad \tilde{\mathbf{e}}_{\mathbf{k}} = (\tilde{u} \pm \tilde{c})^T \tag{29}$$

where

$$\tilde{u}_{i+1/2} = \frac{Q_{i+1}\sqrt{A_i} + Q_i\sqrt{A_{i+1}}}{\sqrt{A_i A_{i+1}}\left(\sqrt{A_{i+1}} + \sqrt{A_i}\right)} \tag{30}$$

$$\tilde{c}_{i+1/2} = \sqrt{\frac{g}{2}\left[\left(\frac{A}{b}\right)_i + \left(\frac{A}{b}\right)_{i+1}\right]} \tag{31}$$

The source terms of the equation system (Eq. 7) are also discretizated using an upwind scheme (García-Navarro et al., 2000):

$$(\tilde{\mathbf{R}}\delta x)_{i+1/2} = \left(\sum_{k+} \tilde{\beta}_k \tilde{\mathbf{e}}_{\mathbf{k}}\right)_{i+1/2} + \left(\sum_{k-} \tilde{\beta}_k \tilde{\mathbf{e}}_{\mathbf{k}}\right)_{i+1/2} \tag{32}$$

in which $\tilde{\beta}_k$ coefficients take the role of $\tilde{\alpha}_k$ ones for the fluxes. Then, the complete discretization of the system becomes:

$$\mathbf{U}_i^{n+1} = \mathbf{U}_i^n - \frac{\delta t}{\delta x}\left[\left(\sum_{k+}\left(\tilde{\lambda}_k\tilde{\alpha}_k - \tilde{\beta}_k\right)\tilde{\mathbf{e}}_{\mathbf{k}}\right)_{i+1/2} + \left(\sum_{k-}\left(\tilde{\lambda}_k\tilde{\alpha}_k - \tilde{\beta}_k\right)\tilde{\mathbf{e}}_{\mathbf{k}}\right)_{i+1/2}\right] \tag{33}$$

4.2 Boundary conditions and stability conditions

In order to solve a numerical problem, it is necessary to impose some physical boundary conditions (BC) at the domain limits. The number of boundary conditions depends

DWESD
7, 27–57, 2014

J. Fernández-Pato and P. García-Navarro

on the flow regime (subcritical or supercritical), so there are four posibilities for a 1-D numerical problem (see Table 1).

In the cases where a pipe junction is present, additional inner boundary conditions are necessary in order to solve the problem. Figure 3 shows an example of a 3 pipe junction.

The water level equality condition is imposed at the junction:

$$h_2(1) = h_3(1) = h_1\left(I^1_{\mathrm{MAX}}\right) \tag{34}$$

Discharge continuity condition is formulated depending on the flow regime:

$$Q_1\left(I^1_{\mathrm{MAX}}\right) = Q_2(1) + Q_3(1), \qquad \text{(sub. junction)} \tag{35}$$

$$Q_2(1) = Q_3(1) = \frac{1}{2}Q_1\left(I^1_{\mathrm{MAX}}\right), \qquad \text{(super. junction)} \tag{36}$$

In a general case, considering N pipes:

$$h_1 = h_2 = \cdots = h_N, \qquad \sum_{i=1}^{N} Q_i = 0 \tag{37}$$

In some cases, a storage well junction is used, so the boundary conditions are modified as follows:

$$h_1 = h_2 = \cdots = h_N = H_{\mathrm{well}}, \qquad \sum_{i=1}^{N} Q_i = A_{\mathrm{well}}\frac{\mathrm{d}H_{\mathrm{well}}}{\mathrm{d}t} \tag{38}$$

where A_{well} and H_{well} are the well top area and depth, respectively. The presented method is explicit, so it requires a control on the time step in order to avoid instabilities. Hence the Courant–Friedrichs–Lewy (CFL) condition is applied in terms of the CFL number:

$$\Delta t_{\max} = \frac{\Delta x}{\max\left(|u| + c\right)}, \qquad \mathrm{CFL} = \frac{\Delta t}{\Delta t_{\max}} \le 1 \tag{39}$$

DWESD
7, 27–57, 2014

A pipe network simulation model

J. Fernández-Pato and P. García-Navarro

5 Test cases

The model is applied to several analytic or experimental test cases in order to evaluate its accuracy.

5.1 Steady state over a bump

Following Murillo et al. (2012) a frictionless rectangular 25 m × 1 m prismatic channel is assumed with the variable bed level $z(8 \le x \le 12) = 0.2 - 0.05(x-10)^2$ and initial conditions given by $h(x,0) = 0.5 - z(x)$ and $u(x,0) = 0$. The test cases simulated are summarized in Table 2.

Figure 4 (a) shows the formation of hydraulic jump that connects both subcritical and supercritical regimes. In the second case, shown in Fig. 4 (b) the connection is made without any shock wave and it can be proved (and numerically checked) that this transition takes place in the highest part of the bump.

5.2 Dam-break

Dam-break is a classical example of non-linear flow with shocks, used to test the accuracy and conservation of the numerical scheme, by comparing with its analytical solution. In the case presented, an initial discontinuity of 1 m : 0.5 m ratio with no friction was considered. Figure 5 shows the good agreement between numerical and analytical solution at the given time.

5.3 Wiggert test case

The experimental case designed by Wiggert (Wiggert, 1972) and widely numerically reproduced (e.g. Kerger et al., 2010; Bourdarias et al., 2007) is a horizontal 30 m long and 0.51 m wide flume. In the middle part a 10 m roof is placed, setting up a closed rectangular pipe 0.148 m in height (see Fig. 6). The Manning roughness coefficient is $0.01\,\mathrm{m}^{-1/3}\mathrm{s}$. A water level of 0.128 m and no discharge are considered as initial

DWESD
7, 27–57, 2014

conditions. Then a wave coming from the left causes the pressurization of the pipe. The imposed downstream boundary conditions are the same values measured by Wiggert (Fig. 7).

Figure 8 shows the numerical results for the four gauges but the experimental comparison is only done for the second one, due to data availability issues. An overall good agreement is observed. Only small numerical oscillations are observed.

5.4 Transient mixed flow

The aim of the next test case is to prove the model in the simulation of large-scale strong transients. It considers a uniform slope (0.1 %) rectangular pipe connected to a downstream valve (León, 2007 and León et al., 2009). The lenght, width and height are 10 km, 10 m and 9.5 m, respectively, and the chosen Manning roughness is 0.015.

As initial condition, a uniform water depth (8.57 m) and discharge ($Q = 240\,\mathrm{m^3\,s^{-1}}$) are assumed. From this state, the downstream valve is closed, generating a shock wave moving upstream and pressurizing the pipe. Figure 9 shows the numerical results obtained for the pressure head at three different times. For this simulation, a 500 cells mesh and a timestep given by CFL=0.5 have beed used. It is clearly observed that the pipe pressure raises gradually with the upwards shockwave movement.

5.5 Pressurized flow transients

A full-pressurized (León, 2007 and León et al., 2009) 10 km flat, frictionless pipe of rectangular section (10 m x 7.853 m) is connected upstream to a water reservoir that guarantees a constant pressure head of 200 m. A closure valve is placed downstream. When the valve is suddenly closed, a waterhammer wave is generated moving upwards. Figure 9 shows the numerical results with CFL = 0.8 and a 500 cells mesh.

This case simulates a completely pressurized pipe, so it is necessary to be very precise in the slot width selection in order to ensure the numerical solution accuracy. A waterhammer speed of $1000\,\mathrm{m\,s^{-1}}$ and a initial flow speed of $2.0\,\mathrm{m\,s^{-1}}$ are assumed.

DWESD
7, 27–57, 2014

J. Fernández-Pato and P. García-Navarro

Following (Eq. 25) condition:

$$c_{\mathrm{WH}} = c \Rightarrow b_s = g\frac{A_{\mathrm{f}}}{c_{\mathrm{WH}}^2} = 0.77\,\mathrm{mm} \tag{40}$$

6 Pipe networks

6.1 Transient flow in a 3-pipe junction

A case proposed in Wixcey (1990) is presented first. We have considered a prismatic main channel (1) dividing into two secondary branches (2 and 3) with the same geometry have been considered, as presented in Fig. 3. The length, width, height and Manning roughness coefficient for all the pipes are 5 km, 1 m, 1 m and 0.01, respectively. The main branch has a slope of 0.002 and the secondary ones 0.001.

Firstly, a steady state has been calculated from the initial conditions:

$$Q_1(i,0) = 0.1\,\mathrm{m^3\,s^{-1}}, \qquad Q_2(i,0) = Q_3(i,0) = 0.05\,\mathrm{m^3\,s^{-1}} \tag{41}$$

$$h_1(i,0) = h_2(i,0) = h_3(i,0) = 0.2\,\mathrm{m} \tag{42}$$

using as boundary condition the inlet discharge:

$$Q_1(1,t) = 0.1\,\mathrm{m^3\,s^{-1}} \tag{43}$$

and zero first derivative boundary condition at the outlet of pipes 2 and 3.

Using this steady state as initial condition for the transient calculation. A triangular function of peak discharge $Q_{\mathrm{MAX}} = 3.2\,\mathrm{m^3\,s^{-1}}$ and a period of 600 s (Fig. 12b) is imposed at the beginning of the pipe 1. Figure 11 shows the numerical results using a 100 cells mesh and a CFL = 0.9 condition.

DWESD
7, 27–57, 2014

A pipe network simulation model

J. Fernández-Pato and P. García-Navarro

6.2 Transient flow in a 7-pipe looped network

In this section a simple looped pipe network (see Fig. 12a) is presented (Wixcey, 1990). Each pipe is closed, squared, 1 m wide and 100 m long. The bed slopes are $S_{0,1} = 0.002$, $S_{0,2} = S_{0,3} = 0.001$, $S_{0,4} = 0.0$, $S_{0,5} = S_{0,6} = 0.001$, $S_{0,7} = 0.002$ and the Manning friction coefficient $n = 0.01$. A first calculation provided the steady state from the following initial conditions:

$$Q_1(i,0) = Q_7(i,0) = 0.1\,\mathrm{m^3\,s^{-1}}$$
$$Q_2(i,0) = Q_3(i,0) = Q_5(i,0) = Q_6(i,0) = 0.05\,\mathrm{m^3\,s^{-1}}$$
$$Q_4(i,0) = 0$$
$$h_1(i,0) = h_2(i,0) = h_3(i,0) = h_4(i,0) = h_5(i,0) = h_6(i,0) = h_7(i,0) = 0.2\,\mathrm{m}$$

and the upstream boundary condition:

$$Q_1(1,t) = 0.1\,\mathrm{m^3\,s^{-1}}$$

Zero first derivative has been used for downwards boundary condition.

Junctions J_1 and J_2 are treated as normal confluences (Eq. 37) and a storage well of 5 m^2 top surface is assumed in junctions W_1 and W_2 (Eq. 38). The steady state is now used as an initial condition for a second calculation. A triangular function of peak discharge Q_{MAX} and a period of 600 s (Fig. 12b) is imposed at the beginning of the pipe 1. The minimum discharge is 0.1 m^3 s^{-1}.

Two different situations were studied. In the first one the peak discharge is fixed to $Q_{\mathrm{MAX}} = 2.0\,\mathrm{m^3\,s^{-1}}$, so the flow remains unpressurized all over the pipe system. In the second case, the maximum discharge is raised to $Q_{\mathrm{MAX}} = 3.0\,\mathrm{m^3\,s^{-1}}$, so pressurization occurs in some points of pipe 1. Figure 13 shows the results for the pressurized case. The results in pipes 3 and 6 have been omitted because of symmetry reasons. The discharge at the center of the pipe 4 is constrantly zero and equal in magnitude but opposite in sign in the symmetric points.

DWESD
7, 27–57, 2014

J. Fernández-Pato and P. García-Navarro

7 Conclusions

The present work leads to the conclusion of the reasonably good applicability of the Preissmann slot model for an estimation of the pressure values in transitory situations between both shallow and pressurized flows. In this case, a small deviation of the ideal value of the slot width introduces an error in the mass and momentum conservation. However, it is clear that wider slots improves the numerical model stability, so it is remarkably important to find an agreement between both facts, in benefit of the numerical results accuracy.

The model takes advanteges of the similarity between the shallow water and pressurized flow equations and provides a way to simulate pressurized pipes treating the system as a open channel in the slot. This fact result in a easier computer implementation of the model because it avoids the numerical complexities that would be required to model separately the pressurized/free-surface portions by water-hammer/shallow-water equations.

The use of an explicit scheme implies a limitation on the time step. This limiting condition increases the calculation time in the pressurized cases, due to the small width of the slot.

It is possible to adapt the method to more realistic systems, like pipe networks which can be punctually pressurized. In these cases, additional internal boundary conditions are necessary in order to represent pipe junctions or storage wells.

References

Bourdarias, C. and Gerbi, S.: A finite volume scheme for a model coupling free surface and pressurised flows in pipes, J. Comput. Appl. Math., 209, 109–131, 2007. 37

Chaudhry, M. H. and Mays, L. W.: Computer modeling of free-surfaces and pressurized flows, Kluwer Academic Publishers, Boston, 741 pp., 1994. 32

García-Navarro, P. and Vázquez-Cendón, M. E.: On numerical treatment of the source terms in the shallow water equations, Comput. Fluids, 29, 951–979, 2000. 30, 35

García-Navarro, P., Alcrudo, F., and Priestley, A.: An implicit method for water flow modelling in channels and pipes, J. Hydraul. Res., 32, 721–742, 1994. 29

Gray, C. A. M.: Analysis of water hammer by characteristics, T. Am. Soc. Civ. Eng., 119, 1176–1189, 1954. 28

Kerger, F., Archambeau, P., Erpicum, S., Dewals, B. J., and Pirotton, M.: An exact Riemman solvrer and a Godunov scheme for simulating highly transient mixed flows, J. Comput. Appl. Math., 235, 2030–2040, 2010. 29, 37

León, A. S.: Improved Modeling of Unsteady Free Surface, Pressurized and Mixed Flows in Storm-sewer Systems, Dissertation, University of Illinois, Illinois, 2007. 38

León, A. S., Ghidaoui, M. S., Schmidt, A. R., and García, M. H.: Application of Godunov-type schemes to transient mixed flows, J. Hydraul. Res., 47, 147–156, 2009. 29, 38

Murillo, J. and García-Navarro, P.: Augmented versions of the HLL and HLLC Riemann Solvers including source terms in one and two dimensions for shallow flow applications, J. Comput. Phys., 231, 6861–6906, 2012. 37

Trajkovic, B., Ivetic, M., Calomino, F., and D'Ippolito, A.: Investigation of transition from free surface to pressurized flow in a circular pipe, Water Sci. Technol., 39, 105–112, 1999. 29

Wiggert, D. C.: Transient flow in free-surface, pressurized systems, J. Hydr. Eng. Div.-ASCE, 98, 11–26, 1972. 37

Wiggert, D. C. and Sundquist, M. J.: Fixed-grid characteristics for pipeline transients, J. Hydr. Eng. Div.-ASCE, 103, 1403–1416, 1977. 28

Wixcey, J. R.: An investigation of algorithms for open channel flow calculations, Numerical Analysis Internal Report, 21, Departament of Mathematics, University of Reading, Reading, 1990. 39, 40

DWESD

7, 27–57, 2014

A pipe network simulation model

J. Fernández-Pato and P. García-Navarro

Table 1. Boundary conditions.

Flow regime and boundary	Number of physical BC to impose
Upstream subcritical flow	1
Upstream supercritical flow	2
Downstream subcritical flow	1
Downstream supercritical flow	0

DWESD
7, 27–57, 2014

J. Fernández-Pato and P. García-Navarro

Table 2. Steady state over a bump.

Test	Upstream Q ($m^3 s^{-1}$)	Downstream h (m)
#1	0.18	0.33
#2	1.53	0.66 (sub)

DWESD
7, 27–57, 2014

J. Fernández-Pato and P. García-Navarro

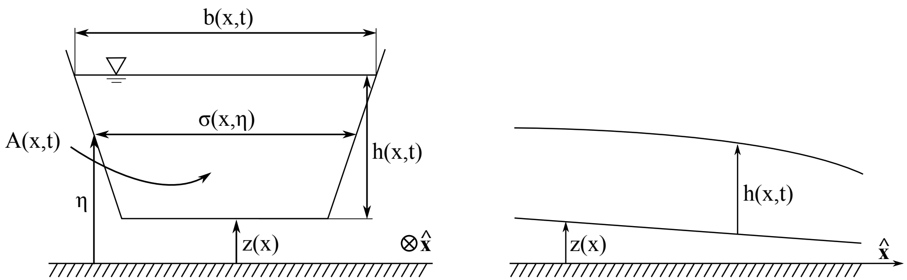

Fig. 1. Coordinate system for shallow water equations.

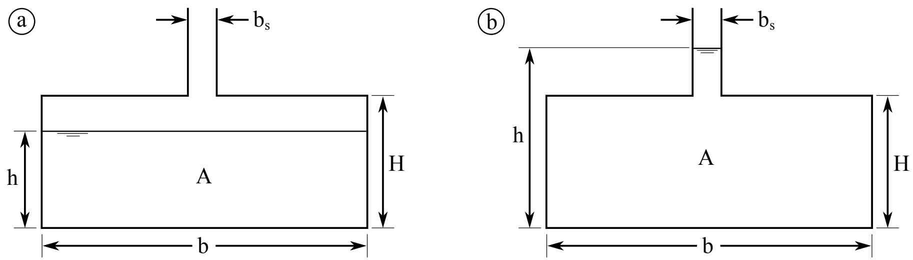

Fig. 2. (a) Pure shallow flow **(b)** Pressurized pipe.

DWESD
7, 27–57, 2014

A pipe network simulation model

J. Fernández-Pato and P. García-Navarro

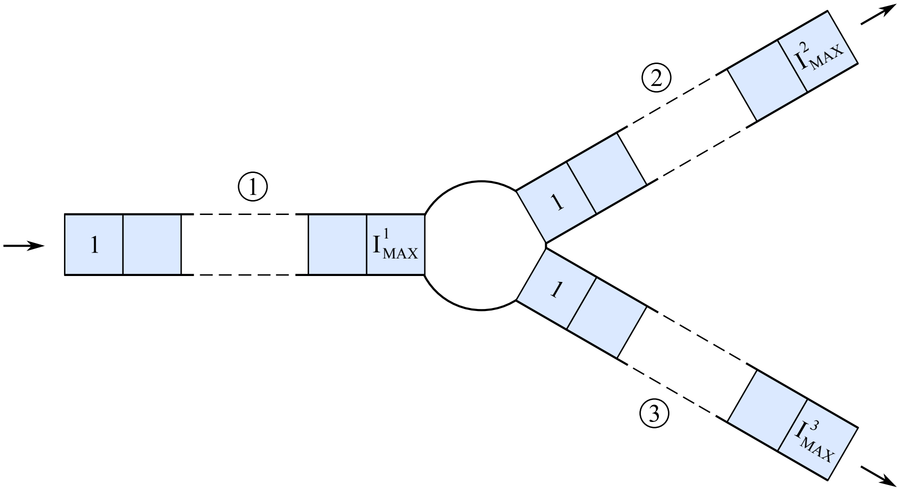

Fig. 3. Example of pipe junction.

Discussion Paper | Discussion Paper | Discussion Paper | Discussion Paper |
DWESD
7, 27–57, 2014
A pipe network simulation model
J. Fernández-Pato and P. García-Navarro

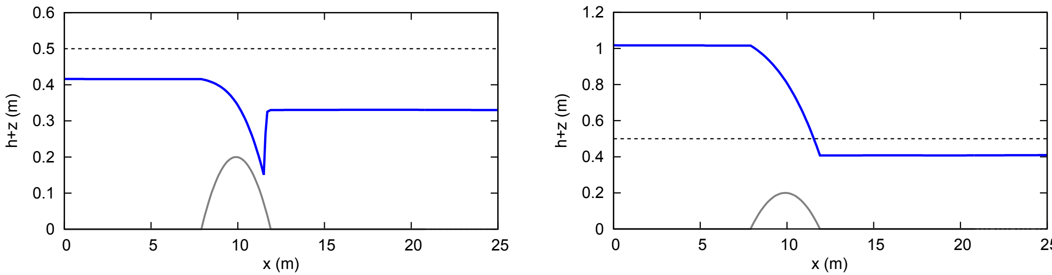

Fig. 4. Steady state over a bump. Initial state (dashed line). Bed level (grey). Numerical solution (blue): **(a)** Test #1; **(b)** Test #2.

DWESD
7, 27–57, 2014

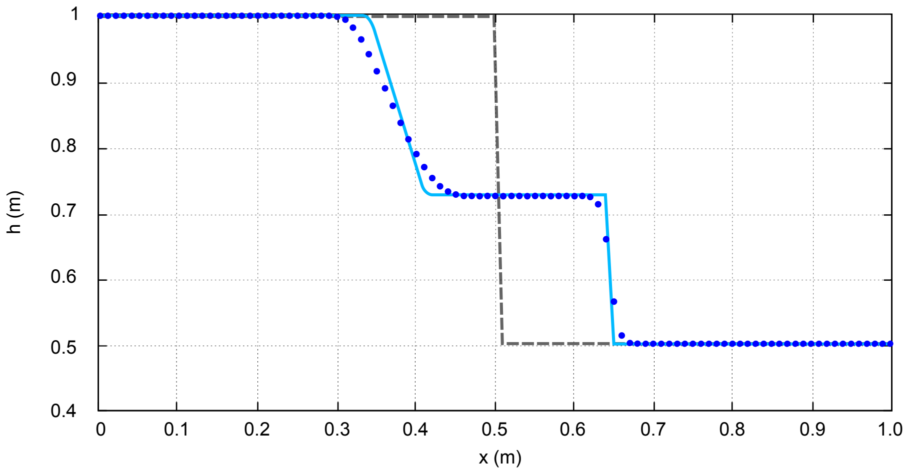

Fig. 5. Dam-break test case. Initial state (dashed line). Numerical results (blue dots). Analytical solution (cyan line).

DWESD

7, 27–57, 2014

A pipe network simulation model

J. Fernández-Pato and P. García-Navarro

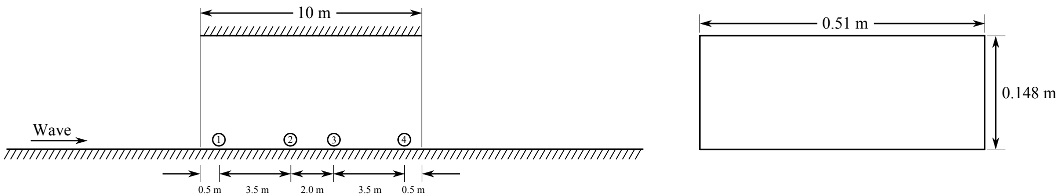

Fig. 6. Wiggert experimental setup.

DWESD
7, 27–57, 2014

J. Fernández-Pato and P. García-Navarro

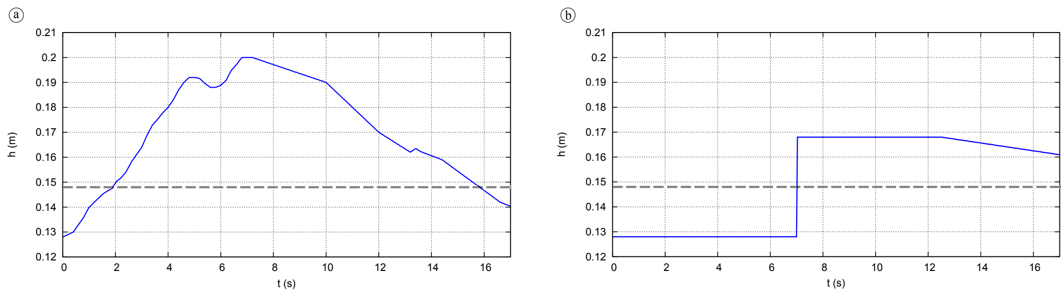

Fig. 7. Upstrem **(a)** and downstream **(b)** pressured head level.

Discussion Paper | Discussion Paper | Discussion Paper | Discussion Paper |

DWESD

7, 27–57, 2014

A pipe network simulation model

J. Fernández-Pato and P. García-Navarro

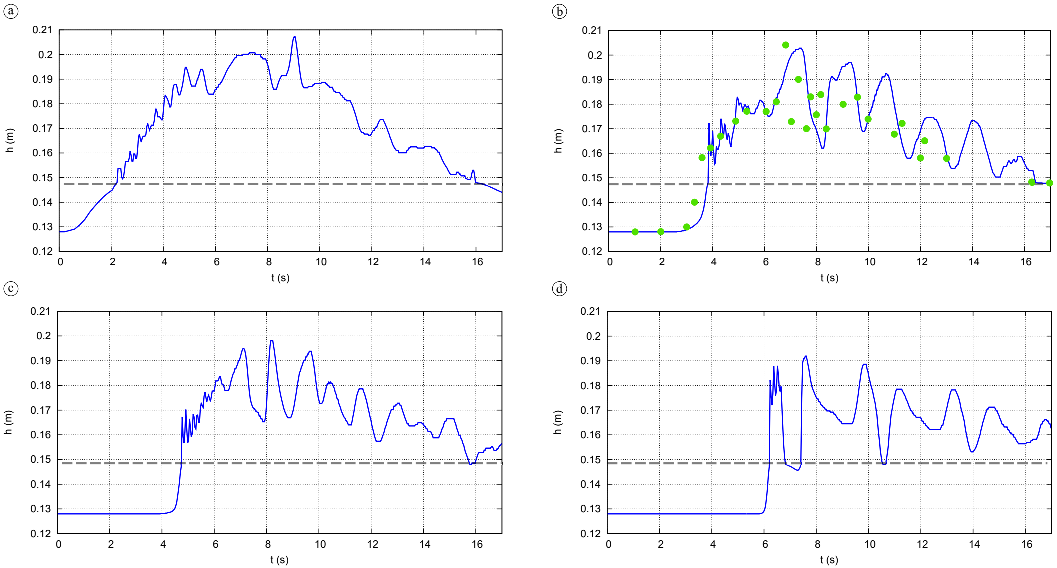

Fig. 8. Comparision between numerical results (blue) and experimental data (green dots) for the Wiggert test case.

DWESD
7, 27–57, 2014

A pipe network simulation model

J. Fernández-Pato and P. García-Navarro

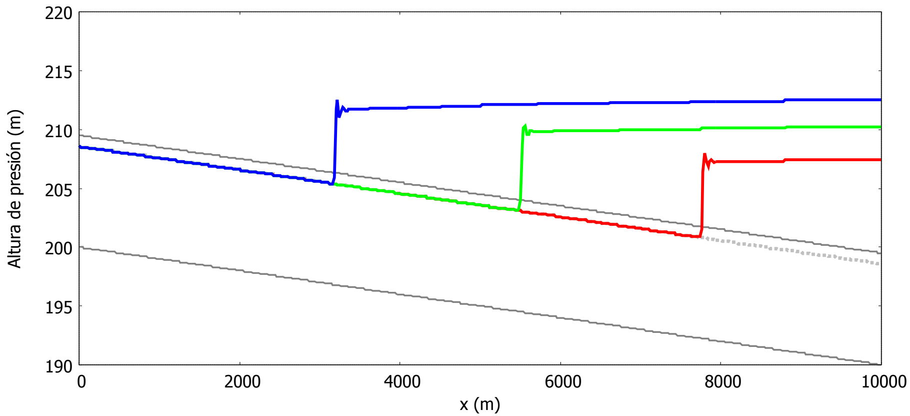

Fig. 9. Shockwave propagation in transient mixed flow at t = 100 s (red), t = 200 s (green) and t = 300 s (blue).

DWESD
7, 27–57, 2014

A pipe network simulation model

J. Fernández-Pato and P. García-Navarro

Title Page
Abstract | Introduction
Conclusions | References
Tables | Figures
◀I | ▶I
◀ | ▶
Back | Close
Full Screen / Esc
Printer-friendly Version
Interactive Discussion

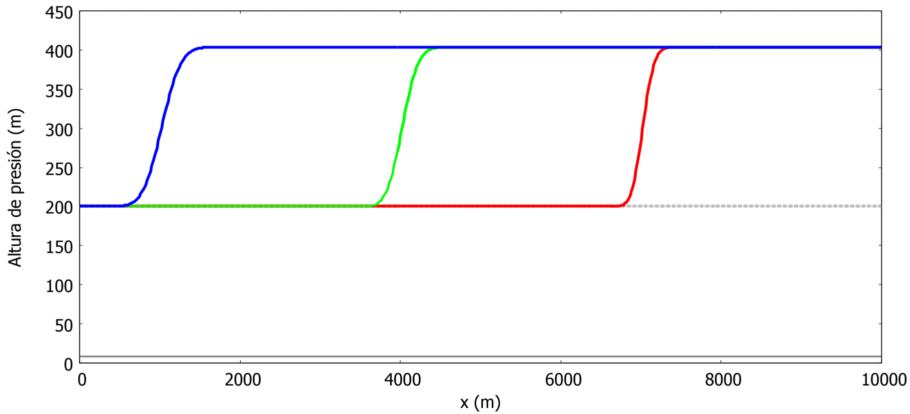

Fig. 10. Waterhammer simulation. Pressured head at $t = 3$ s (red), $t = 6$ s (green) and $t = 9$ s (blue).

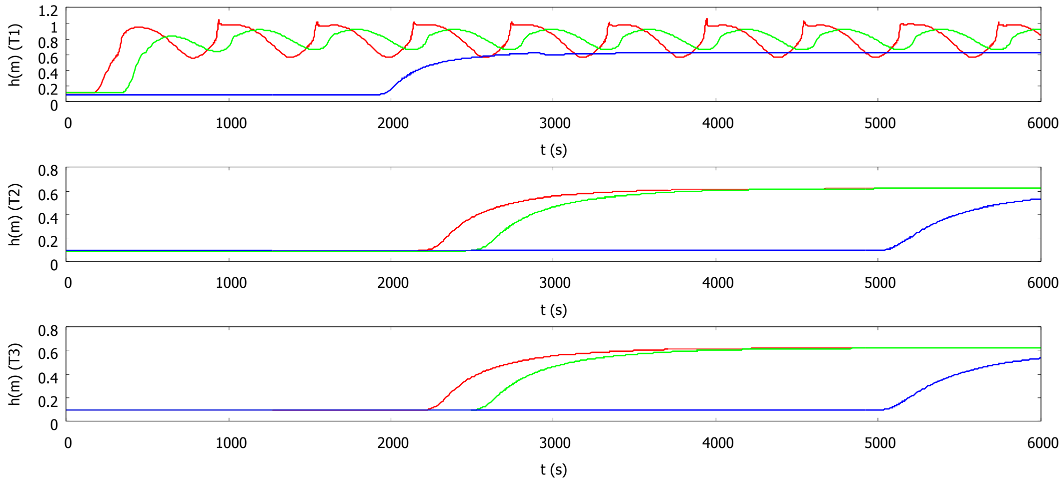

Fig. 11. Pressurized transient in a pipe junction. Pressured head vs. time $x = 500\,\mathrm{m}$ (red), $x = 1000\,\mathrm{m}$ (green) and $x = 5000\,\mathrm{m}$ (blue).

DWESD

7, 27–57, 2014

A pipe network simulation model

J. Fernández-Pato and P. García-Navarro

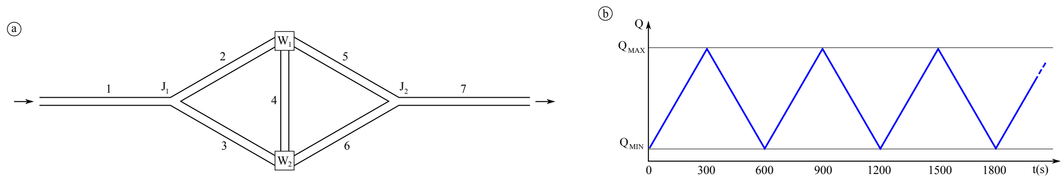

Fig. 12. (a) Scheme of the looped pipe network; **(b)** Triangular inlet hydrograph in the pipe 1.

DWESD
7, 27–57, 2014

Title Page
Abstract Introduction
Conclusions References
Tables Figures
◀ ▶
Back Close
Full Screen / Esc
Printer-friendly Version
Interactive Discussion

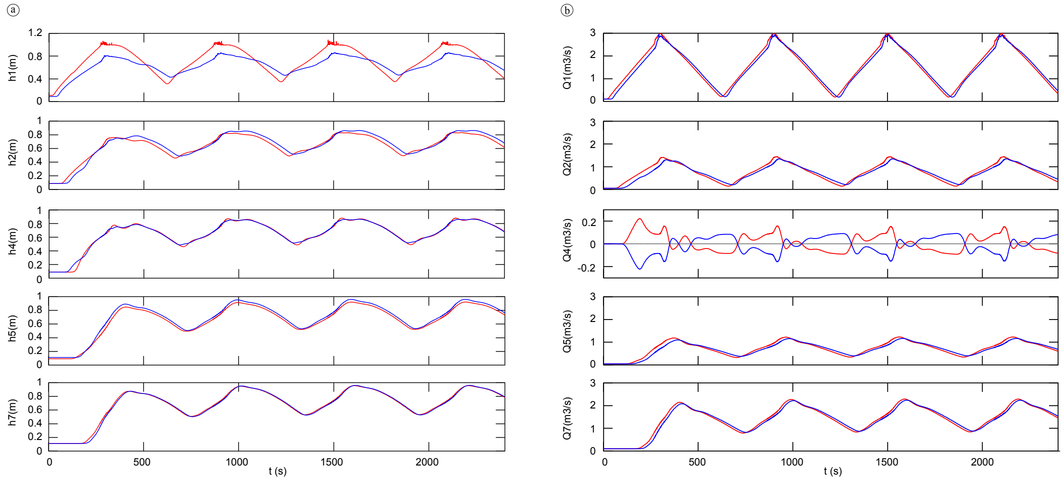

Fig. 13. Time histories at grid points $i = N/2$ (red) and $i = N$ (blue) for punctually pressurized flow: **(a)** water depth; **(b)** discharge. The discharge for pipe 4 is recorded at locations $i = 1$ (red), $i = N/2$ (grey) and $i = N$ (blue).

DWESD
7, 27–57, 2014

A pipe network simulation model

J. Fernández-Pato and P. García-Navarro